ORIGINAL RESEARCH

Effects of Gabexate Mesylate on the Gut Microbiota and Metabolomics in Rats with Sepsis

Wenju Sun[1],*, Yuqing Cui[1],*, Xiaojuan Zhang[1],*, Yuze Wang[1], Zihao Zhang[2], Xianfei Ding[1], Huoyan Liang[1], Dong Wang[1], Yali Sun[1], Shaohua Liu[1], Xiaoguang Duan[1], Yibin Lu[3], Tongwen Sun[1]

[1]General ICU, The First Affiliated Hospital of Zhengzhou University, Henan Key Laboratory of Critical Care Medicine, Zhengzhou Key Laboratory of Sepsis, Henan Engineering Research Center for Critical Care Medicine, Zhengzhou, 450052, People's Republic of China; [2]Department of Clinical Medicine, Sanquan College of Xinxiang Medical University, Xinxiang, 453003, People's Republic of China; [3]Department of Critical Care Medicine, Xinyang Hospital Affiliated to Zhengzhou University, Xinyang, 464000, People's Republic of China

*These authors contributed equally to this work

Correspondence: Tongwen Sun, General ICU, The First Affiliated Hospital of Zhengzhou University, Henan Key Laboratory of Critical Care Medicine, Zhengzhou Key Laboratory of Sepsis, Henan Engineering Research Center for Critical Care Medicine,Zhengzhou, Henan Province, 450052, People's Republic of China, Email suntongwen@163.com

Background: Sepsis is a life-threatening organ dysfunction caused by a dysregulated host response to infection. However, there is still no single drug that could reduce septic mortality. Previous studies have reported gabexate mesylate (GM) significantly reduced serum inflammatory factors, alleviated sepsis-induced lung injury and improved clinical outcomes. This study aimed to combine with microbiome sequencing and metabolomics analysis to explore the effects of GM administration in septic rats.

Methods: Sixty SD rats were randomly divided into the sham control (SC), cecal ligation and puncture (CLP), and GM injection (GM) groups. The mortality was measured and colonic feces were collected to examine the gut microbiota and metabolism 24 h after the procedure. The lung tissues were collected for hematoxylin-eosin staining.

Results: We observed the relative abundance of Pygmaiobacter, which contributed to short-chain fatty acids (SCFAs) promotion, Lactobacillus and Erysipelotrichaceae UCG-003 increased in the GM-treated rats, while Escherichia–Shigella and Akkermansia decreased compared to the sepsis-induced lung injury group. Furthermore, these 3 metabolites including Palmitoylethanolamide, Deoxycholic acid and Chenodeoxycholic acid correlated significantly to CLP- and GM-rich genus ($P < 0.05$). Besides, the lung tissues of CLP group showed more severe inflammatory infiltration and edema, and the mortality rate in the CLP group (10/20) was significantly higher than in the SC group (0/20) ($P < 0.001$) and GM group (4/20) ($P < 0.05$).

Conclusion: Our findings showed that GM attenuated sepsis-induced lung injury rats and regulated metabolites related to gut microbiota, which may provide an effective treatment for sepsis patients.

Keywords: sepsis, gabexate mesylate, gut microbiota, metabolomics, rats

Introduction

Sepsis affects the lives and health of millions of people worldwide annually. Sepsis results in life-threatening organ dysfunction caused by loss of control over infection.[1] One of the main causes of organ failure in sepsis is the inflammatory response due to infection.[2] According to statistical data, the sepsis mortality rate in hospitalized patients is 26.7%, and the sepsis mortality rate in the intensive care unit is 41.9%.[3] Despite recent decades, no treatment has been approved for sepsis other than antibiotics and supportive care.[4] Finding a promising drug to reduce sepsis mortality remains a serious challenge.

Gabexate mesylate (GM) is a non-peptidic serine protease inhibitor,[5] which can inhibit the coagulation cascade and be used clinically as an anticoagulant in patients with acute pancreatitis[6] and disseminated intravascular coagulation (DIC).[7] Abnormal coagulation can lead to a large increase in plasma plasminogen activator inhibitor 1 (PAI-1)[8] level, the formation of microthrombi and pulmonary vascular injury.[9] GM can also inhibit various serine proteases produced during inflammation,[10] which has a certain

anti-inflammatory effect. It directly inhibited the activation of NF-κB in lipopolysaccharide (LPS)-stimulated macrophages and human monocytes, resulting in decreased production of inflammatory cytokines such as TNF-α, IL-6 and high mobility group protein 1 (HMGB1).[11] Besides, GM has a protective effect in acute lung injury caused by endotoxin,[12] ischemia/reperfusion,[13] and smoke inhalation.[14] It alleviated LPS-induced coagulation abnormalities and pulmonary vascular injury by inhibiting TNF-α production.[12] Vitro experiments demonstrated that GM inhibited the function of activated neutrophils. However, inflammatory mediators produced by neutrophils, such as granulocyte elastase and superoxide free radicals, as well as neutrophil aggregation, are associated with pulmonary vascular injury.[15] It also attenuates LPS-induced lung injury by inhibiting the expression of leukocyte adhesion molecules in endothelial cells.[16] Studies have found that GM indirectly inhibits the expression of HMGB1 and reduces lung injury by inhibiting PAI-1 and protease activated receptor 2 (PAR-2).[11] Since PAI-1 levels are associated with the severity and prognosis of multiple organ failure in patients with sepsis, GM can also partially prevent the development of organ dysfunction through anticoagulation.[17] Some studies have shown that GM significantly reduced the neutrophil infiltration scores in lung, liver and kidney, and alleviated organ dysfunction in septic rats.[18,19] But the potential mechanisms by which GM can be used for sepsis treatment have not been elucidated.

The gut is the main origin of microorganisms that lead to sepsis. Gut microbiota regulates the homeostasis of healthy hosts through immune function and intestinal barrier.[20] Decreased diversity of the microbiome,[21] thinning of the gut mucus layer and increased gut permeability, allow pathogens to thrive in the gut lumen.[22] Several studies reported that the gut microbiota dysbiosis increased susceptibility to sepsis[23] and organ dysfunction, which associated with sepsis progression.[24] Gut bacterial content determines the severity of systemic damage in sepsis, suggesting that dysbiosis also affects sepsis prognosis.[25] Increasing evidence indicates that gut microbiota plays a key role in pulmonary immunity and is associated with airway homeostasis.[26] For example, intestinal microbes can enhance host defense against pneumonia through increased IL-17 and upregulation of granulocyte-macrophage colony-stimulating factor (GM-CSF) signaling.[27] The gut microbiota derived metabolites, such as short-chain fatty acids (SCFAs), can induce the production of immune cells and cytokines, which subsequently enter the systemic circulation to regulate immune and inflammatory responses in the lung.[28] Lung SCFA levels are dependent on functional gut microbiota, and SCFA (propionic acid) reprograms the metabolism of alveolar macrophages. In addition, oral SCFA can reduce airway hyperresponsiveness and increase regulatory T cells in bronchoalveolar lavage fluid.[29] It can target alveolar macrophages to remotely influence lung immune responses, modulating asthma[30] and respiratory infections.[31] However, SCFA (acetate) supplementation reduced the bacterial burden after influenza attack, alleviated pulmonary pathology and improved survival.[32]

The gut microbiota plays a key role in sepsis and septic shock, and gut dysbiosis could contribute to the onset of sepsis by producing harmful metabolites and altering host physiological processes. Microbe-derived SCFAs also contribute to intestinal mucosal homeostasis and enhance clearance of pathogenic microorganisms by immune cells such as macrophages.[33] These bacterial metabolites are essential elements of the microbiota–host interaction. Dysbiosis leads to reduced levels of gut microbiota-derived SCFAs, which may be due to reduction of Parabacteroides, Prevotella, and Bifidobacterium abundance and further triggers immune cascades in the respiratory tract.[34] Limited evidence suggests that microbiome-based therapies, including probiotics and fecal microbiota transplantation, may reduce sepsis risk and improve septic outcomes.[35,36]

In this study, we aimed to investigate the effect of GM on regulation of the gut microbiota, identify the metabolites involved and explore the protective effect on sepsis. Since the current treatment of sepsis is facing huge challenges, our findings may provide evidence for new therapeutic strategies for sepsis.

Materials and Methods

Instruments and Reagents

The following instruments and reagents were used: bench-type high-speed centrifuge (Eppendorf), PCR instrument (Bio-Rad), electrophoresis instrument (Tanon), Illumina NovaSeq sequencer (Illumina), Vanquish ultra-high-performance liquid chromatograph (Thermo Fisher Scientific), high-resolution mass spectrometry Q Exactive HFX (Thermo Fisher Scientific), Column ACQUITY UPLC HSS T3 (2.1 mm × 100 mm, 1.7 μm) (Waters); Magnetic Bead Method Soil and Fecal DNA Extraction Kit

(Tiangen Biochemical Technology [Beijing] Co., Ltd., DP712), Phusion® High-Fidelity PCR Master Mix with GC Buffer (Thermo Fisher Scientific, F532S), Phusion® High-Fidelity DNA polymerase (New England Biolabs, M0530S) NEB Next® Ultra DNA Library Prep Kit (Illumina, E7370L), methanol (CNW Technologies, CAS 67–56-1), acetonitrile (CNW Technologies, CAS 75–05-8), ammonium acetate (Sigma-Aldrich, CAS 631–61-8), ammonia (Fisher Chemical, CAS 1336–21-6), Ultra Pure Water (Watsons) and GM (0.1 g, Changzhou Siyao Pharmaceuticals Co., Ltd.).

Experimental Animals and Grouping

Sixty 6–8-week-old adult male Sprague–Dawley (SD) rats weighing 200–250 g (https://www.vitalriver.com/). All rats were housed in a 12/12-h day and night animal room for a week before the experiment and allowed to eat and drink ad libitum. The temperature in the animal room was controlled from 20 °C to 25 °C, and the relative humidity was controlled from 40% to 60%. SD rats were randomly divided into sham operation control (SC) group, sepsis after cecal ligation and puncture (CLP) group, and intraperitoneal injection of GM 1 h after CLP group. The establishment of the CLP model was based on our previous studies.[37,38] The rats were weighed and anesthetized by intraperitoneal injection of 30 mg/kg pentobarbital. A 2-cm incision was made on the midline of the abdomen, the cecum was exposed, and the feces were squeezed in the cecum to the free end. It was ligated at the middle and lower one-third of the cecum, and an 18-G needle was used to puncture the middle of the cecal ligation. After the puncture, a small amount of feces is squeezed out, and the cecum is returned to the original position of the abdomen. The muscle and skin layer were sutured with No. 5 and No. 3 surgical sutures, respectively. Immediately after the procedure, subcutaneous injection of 50 mL/kg of warm saline was used for resuscitation, and the rats were irradiated with warm light for 30 min. The SC group underwent the same procedure without ligation and puncture. The GM group received intraperitoneal injection of GM (40 mg/kg) 1 h after CLP. One hour after CLP, rats in the SC and CLP groups were intraperitoneally injected with normal saline. The experiments were conducted according to the guidelines established by the National Institutes of Health (http://grants1.nih.gov/grants/olaw/) and approved by the Ethics Committee of the First Affiliated Hospital of Zhengzhou University.

Sample Collection

The survival rate of the rats was determined 24 h after the operation. Colonic feces of the surviving rats in each group (two tubes of samples were obtained from each rat) were squeezed and placed into 2-mL cryopreservation tubes separately and stored in liquid nitrogen. The perfused lung tissues were collected, and the perfusion procedure was performed similar to that in the previous study.[37] Lung tissues were fixed with 4% paraformaldehyde, embedded in paraffin overnight, stained with hematoxylin and eosin (HE), and observed under a microscope (Olympus, Japan).

Fecal DNA Extraction and High-Throughput 16S rRNA Sequencing

DNA was extracted from the fecal samples using sodium dodecyl sulfate; then, the DNA was diluted to 1 ng/μL sterile water, and the primers were 341F:CCTAYGGGRBGCASCAG and 806R:GGACTACNNGGGTATCTAAT, targeting the 16S V3–V4 region. The DNA purity and concentration were verified by electrophoresis in 2% agarose gel and purified by magnetic spheres. Library construction was qualified and sequenced on NovaSeq 6000.

16S rRNA Sequencing Data Analysis

The original data were spliced and filtered to obtain valid data. Based on the valid data, the clusters of operating taxonomic units (OTUs) and species classification were analyzed with 97% consistency. Subsequently, the species was recorded on the representative sequence of each OTU to obtain species-related information and species-based abundance distribution. Chao1, ACE, Shannon, Simpson, Good's coverage, and phylogenetic diversity (PD) whole tree indices were calculated using QIIME software. Principal component analysis (PCA) was performed using the ade4 package and ggplot2 package of R software (version 2.15.3); principal coordinate analysis (PCoA) was performed using WGCNA and stats and ggplot2 packages; and R software was used to draw the rarefaction curve and analyze the differences between the groups of α- and β-diversity. Parametric and nonparametric tests were used in the data analysis, t-test and Wilcoxon test were used for two-group comparison, and Tukey's and Wilcoxon tests were used for three-group comparison. Linear

discriminant analysis (LDA) effect size (LEfSe)[39] was performed by comparing two or more groups and examining markers that are statistically different between groups. LEfSe used the Kruskal–Wallis rank-sum test to detect characteristics with significantly different abundance levels among the specified taxa, and LDA was performed to estimate the effect size, emphasizing statistical significance and biological relevance. Tax4Fun was used to predict the microbiota function. Correlations between different species and functional pathways were calculated using Spearman rank correlations, and correlations were presented using a heatmap.

Fecal Sample Preparation for Metabolomic Analysis

Moreover, 25 mg of thawed stool sample was obtained and mixed with 500 μL of extract (methanol: acetonitrile: water = 2:2:1). Then, 20 μL of 0.3 mg/mL 2-chloro-D-phenylalanine was added. All samples were ground and ultrasonically extracted in ice water for 5 min, and the steps were repeated two to three times and allowed to stand at −40 °C for 1 h. Then, the supernatant was used in the analysis by centrifugation at 12,000 rpm for 15 min at 4 °C. Each 20 μL of sample was mixed to obtain a quality control (QC) sample, and 200 μL of QC sample was collected for QC analysis.

LC-MS Metabolomics-Based Data Acquisition

Chromatographic separation of metabolites was performed using ultra-high-performance liquid chromatography (UPLC) and UPLC BEH Amide column (2.1 mm × 100 mm, 1.7 μm) (autosampler temperature, 4°C; injection volume, 2 μL). Liquid chromatography phase A consisted of an aqueous phase containing 25 mmol/L ammonium acetate and 25 mmol/L ammonia water, and phase B contained acetonitrile. The conditions of the ionization source of the electrospray were set as follows: the flow rate of the gas in the sheath is 30 Arb, the flow rate of the auxiliary gas is 25 Arb, and the capillary temperature is 350°C. The resolution of mass spectrometry for primary information acquisition was set to 60,000, and secondary information acquisition was set to 7500. The collision energy was 10/30/60 in normalized collision energy mode, and the spray voltage was 3.6 kV (positive) or −3.2 kV (negative). The Thermo Q Exactive HFX mass spectrometer collects mass spectral data as raw data.

Metabolomics Data Analysis

After processing the raw data for peak identification, peak extraction, peak alignment, and integration, a dataset containing mass-to-charge ratio, retention time, and peak intensity was obtained. Then, the data were preprocessed, normalized and matched with an internal mass spectrometry database (BiotreeDB V2.1), and metabolites were annotated with a cutoff point of 0.3. Unsupervised PCA was performed to visualize metabolic changes between groups. Discriminant analysis of orthogonal partial least squares (OPLS-DA) was applied to visualize the maximum difference between the two groups. The variable importance in projection (VIP) was calculated, and a high VIP indicated that the metabolite has a large contribution to the grouping. Data were analyzed using one-way analysis of variance and Tukey's post hoc test (SPSS software version 21.0, Chicago, IL). Metabolites with VIP > 1 and $P < 0.05$ were selected as differential metabolites. Heatmaps were used to show trends in differential metabolites. Pathway analysis was performed using MetaboAnalyst 3.0, which is based on database sources, including the KEGG database (http://www.genome.jp/kegg/) and Human Metabolome Database (https://hmdb.ca/).

Results
Composition of the Gut Microbiota in the Three Groups

The rarefaction curve of each sample was close to saturation, the amount of sequencing data was reasonable, and the sequencing depth was sufficient (Figure 1A). Sample valid sequences with 97% identity were clustered into OTUs. The gut microbiota was annotated with representative OTUs, with a total of 2126 OTUs. Moreover, 660, 616 and 850 OTUs were identified in the SC, CLP, and GM groups, respectively, of which 495 OTUs were shared by three groups (Figure 1B). In the phylum-level gut microbiota, the predominant phyla in the SC and GM groups were Firmicutes, Proteobacteria, and Verrucomicrobiota in the CLP group (Figures 1C). The Firmicutes–Proteobacteria ratio was significantly decreased in the CLP group (Figures 1D). The predominant genera in the SC and GM groups were Lactobacillus, Ruminococcus, and Blautia. The predominant genera in the CLP group were Escherichia–Shigella, Akkermansia, and Enterococcus (Figure 1E).
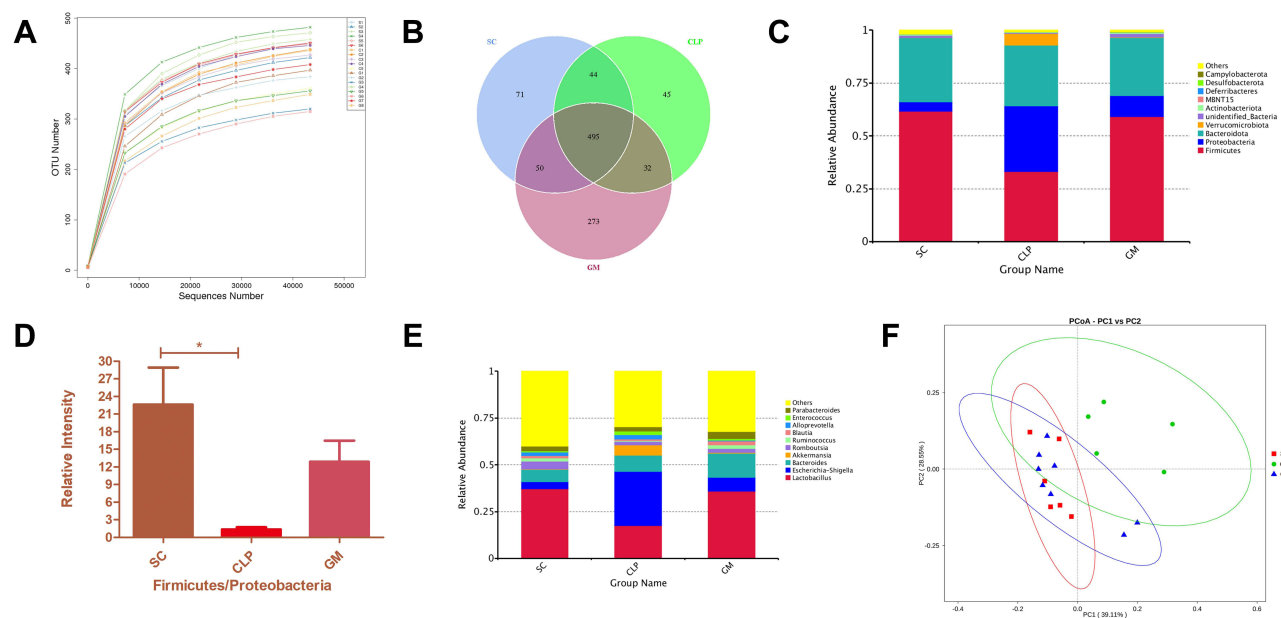
Figure 1 Effect of GM on the gut microbiota of rats with sepsis. (**A**) Rarefaction curves plotted for each sample. (**B**) The Venn diagram of the OTUs of each group. (**C**) Histogram of relative abundance of top ten species at the phylum level. (**D**) The ratio of Firmicutes to Proteobacteria in the SC, CLP, and GM groups; *compared with the CLP group, $P < 0.05$. (**E**) Relative abundance of the top ten species at the genus level. (**F**) PcoA analysis based on weighted Unifrac distance.

α-Diversity Analysis

The Simpson index represented the diversity and evenness of species distribution. The Wilcoxon rank-sum test showed that the diversity and evenness (Simpson index) of species distribution in the SC and GM groups were higher than those in the CLP group. The Shannon index, which measures the total number of microbial communities and their proportions, was also higher in the SC and GM groups than in the CLP group. The Chao1 index and ACE were used to evaluate the total number of species and OTUs, respectively. Interestingly, the Chao1 index and ACE were the lowest in the GM group. Good's coverage index represents the sequencing depth. Good's coverage rates of the three groups were all greater than 99.8%, indicating that the sequencing depth of the gut microbiota was ideal. The PD whole tree index represents the genetic relationship of the species in the community. The PD whole tree index in the SC and GM ($P < 0.01$) groups was higher than in CLP group (Table 1).

β-Diversity Analysis

To assess the degree of similarity between microbial communities, conducted sampling comparative analysis (β-diversity analysis) for different groups. The PCoA results showed that samples from the SC, CLP, and GM groups formed three distinct clusters, among which samples from the SC and GM groups tended to cluster together, indicating that the two groups had similar species composition. The CLP group was far away, indicating that it had a larger community difference compared with the SC and GM groups (Figure 1F). Through ANOSIM and Adonis nonparametric tests, the obtained value of Pr (>F) is $P < 0.05$. It indicated a high degree of sample difference and statistical significance of PCoA analysis results between SC-CLP and CLP-GM groups. The results are shown in Supplementary Table 1 and Supplementary Table 2.

Table 1 Diversity Analysis of a Single Sample with Different Groups Under the 97% Consistency Threshold

Group	Simpson	Shannon	Chao1	ACE	Goods Coverage	PD Whole Tree
SC	0.947	5.711	475.762	479.040	>99.8%	33.920
CLP	0.873	4.911	428.522	436.556	>99.8%	28.936
GM	0.903	4.993	408.385	413.499	>99.8%	39.722**

Notes: Comparison with CLP, **$P < 0.01$.

Differential Microbiota Analysis in the SC, CLP, and GM Groups

To identify the specific microbiota associated with the SC, CLP, and GM groups, we used LEfSe analysis. According to the criteria of LDA > 4 and $P < 0.05$, the differential microbiota was screened. There are three differential genera, namely, Lactobacillus, Romboutsia, and Escherichia–Shigella, between the CLP and SC groups (Figure 2A). Similarly, there were five differential genera between the CLP and GM groups, namely, Lactobacillus, Pygmaiobacter, Erysipelotrichaceae_UCG_003, Escherichia–Shigella, and Akkermansia (Figure 2B). The only differential genera between the SC group and GM group was Parasutterella (Figure 2C).

Correlation Analysis of Genera Between the CLP and GM Groups

The gut microbiota is interconnected to maintain homeostasis, and studying the interactions between different genera contributes to finding the important role of microbiota of the CLP and GM groups ($P < 0.05$). Notably, the GM-enriched genera had higher associations than the CLP group-enriched genera. Akkermansia was strongly positively correlated with Desulfovibrio. Lachnospiraceae UCG-006 closely related to lipid metabolism was strongly negatively correlated with Lactobacillus in the CLP group. Moreover, Lactobacillus was strongly negatively correlated with Desulfovibrio, which was considered to be toxic to the intestinal epithelium (Supplementary Figure 1). In the GM group, Ruminococcus was strongly negatively correlated with common opportunistic pathogens Escherichia–Shigella and Enterobacteria, and Candidatus Saccharimonas with anti-inflammatory property was strongly negatively correlated with Escherichia–Shigella (Supplementary Figure 2). The enriched Muribaculum in the CLP group was strongly negatively correlated with the enriched Lactobacillus in the GM group and strongly positively associated with the enriched Lachnospiraceae UCG-006 in the CLP group. The enriched Akkermansia in the CLP group was strongly positively correlated with Terrisporobacter, Proteus, and Odoribacter. Candidatus Saccharimonas enriched in the GM group was strongly negatively correlated with Escherichia–Shigella enriched in the CLP group (Supplementary Figure 3).

Functional Alterations of GM on Gut Microbiota in the CLP Group

To characterize the functional alterations of gut microbiota following GM application in rats with sepsis, we used Tax4Fun to analyze 16S rRNA and predicted functional composition profiles. Eighteen pathways were differentially enriched ($P < 0.05$)
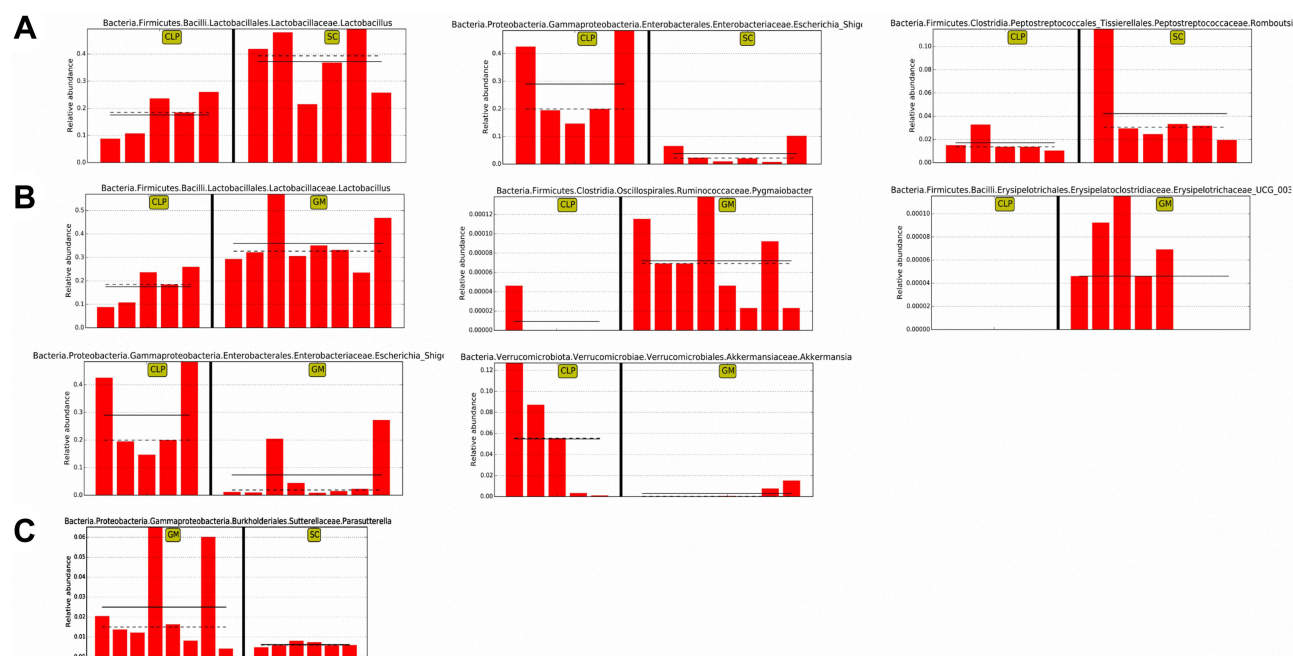

Figure 2 Comparison of abundances of biomarkers with statistical differences in different groups. (**A**) Linear discriminant analysis (LDA) relative abundance map of differential bacterial genera between the CLP and SC groups. The columns represent the relative abundance of each sample, while the solid and dotted lines represent the mean and median, respectively. (**B**) Linear discriminant analysis (LDA) relative abundance map of differential bacterial genera between the CLP and GM groups. (**C**) Linear discriminant analysis (LDA) relative abundance map of differential bacterial genera between the SC and GM groups.

between the CLP and GM groups (Supplementary Figure 4). Then, we investigated the correlation between different species (n = 27) and KEGG pathways (n = 44) using Spearman correlation analysis (Student's t-test) (Supplementary Figure 5). CLP-enriched Akkermansia was negatively correlated with phospholipase D signaling pathway and carbohydrate metabolism signaling pathway. GM-enriched Lactobacillus is associated with several pathways, such as cell cycle, tight junction, phospho-transferase system, isoflavone biosynthesis, caffeine metabolism, thyroid hormone synthesis, mineral absorption, and cellular motility and secretion, and positively correlated with transport and cancer pathways. GM-enriched Ruminococcus was positively correlated with amino sugar and nucleotide sugar metabolism, while Lactobacillus was negatively associated with apoptosis, lipopolysaccharide biosynthesis, steroid hormone biosynthesis, transport, sphingolipid metabolism, and pathways in cancer, fluid shear stress, and atherosclerosis. The dominant Phascolarctobacterium in the CLP group was positively correlated with G protein coupled receptors. Moreover, the dominant Colidextribacter in the CLP group was positively correlated with polyketide sugar unit biosynthesis, terpomycin biosynthesis, and N glycan biosynthesis (Supplementary Figure 6).

Metabolite Analysis of the SC, CLP, and GM Groups

Six samples and a QC sample were run during the running process. The aggregation of the QC samples was good, indicating that the method was stable and experimental data had high quality (Supplementary Figure 7). The total ion chromatograms of the SC, CLP, and GM groups were observed (Supplementary Figure 8). In PCA, the SC group was closer to the GM group and was significantly separated from the CLP group (Figures 3A and D). Using OPLS-DA, the SC, CLP and CLP, GM groups can be divided according to their metabolic differences, and the distinction is significant (Figures 3B and C, 3E and F).

Differential Metabolite Identification

Multivariate statistical analysis was used to screen differential metabolites (VIP > 1.0 and $P < 0.05$). In the positive ion mode, the SC group had 28 differential metabolites compared with the CLP group, eight were significantly upregulated in the SC group, and 20 were significantly downregulated in the SC group (Figure 4A). The GM group had 26 differential metabolites compared with the CLP group: 13 were significantly upregulated and 13 were significantly downregulated (Figure 4B). In the negative ion mode, the SC group had 17 differential metabolites compared with the CLP group: 12 were significantly upregulated and 5 were significantly downregulated (Figure 4C). The GM group had 20 differential metabolites compared with the CLP group: 16 were significantly upregulated and 4 were significantly downregulated (Figure 4D). There were 15
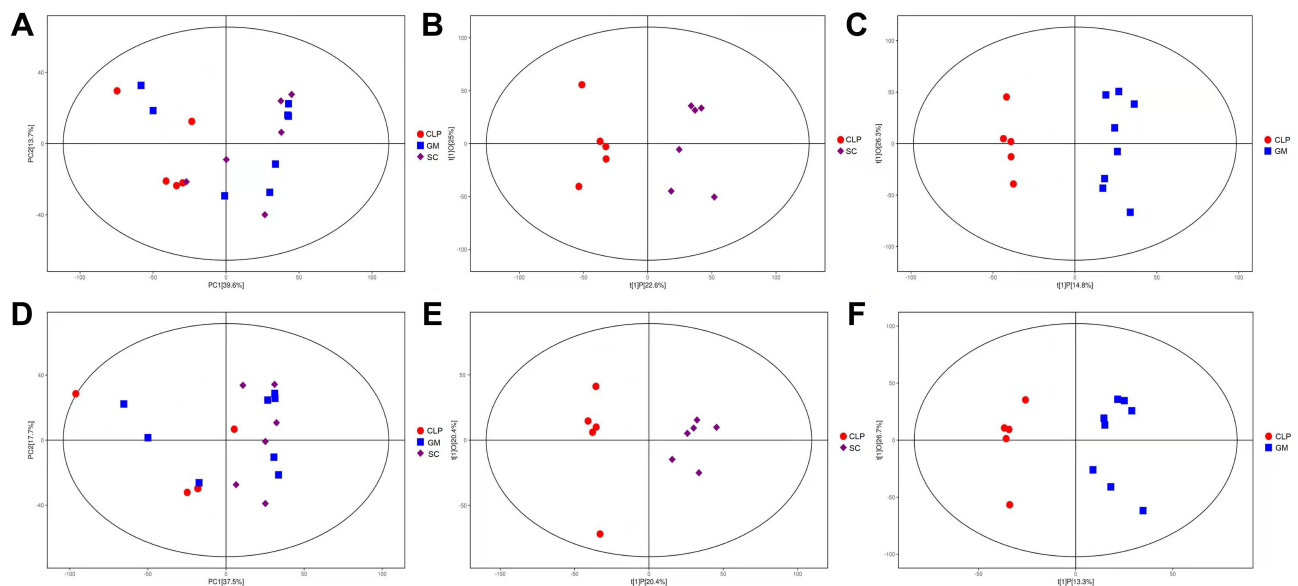

Figure 3 (**A–C**) represent positive ion mode; (**D–F**) represent negative ion mode. (**A** and **D**) represent the PCA diagrams of the SC, CLP and GM groups. (**B** and **E**) represent the OPLS-DA diagrams of the SC and CLP groups. (**C** and **F**) represent the OPLS-DA diagrams of the GM and CLP groups.
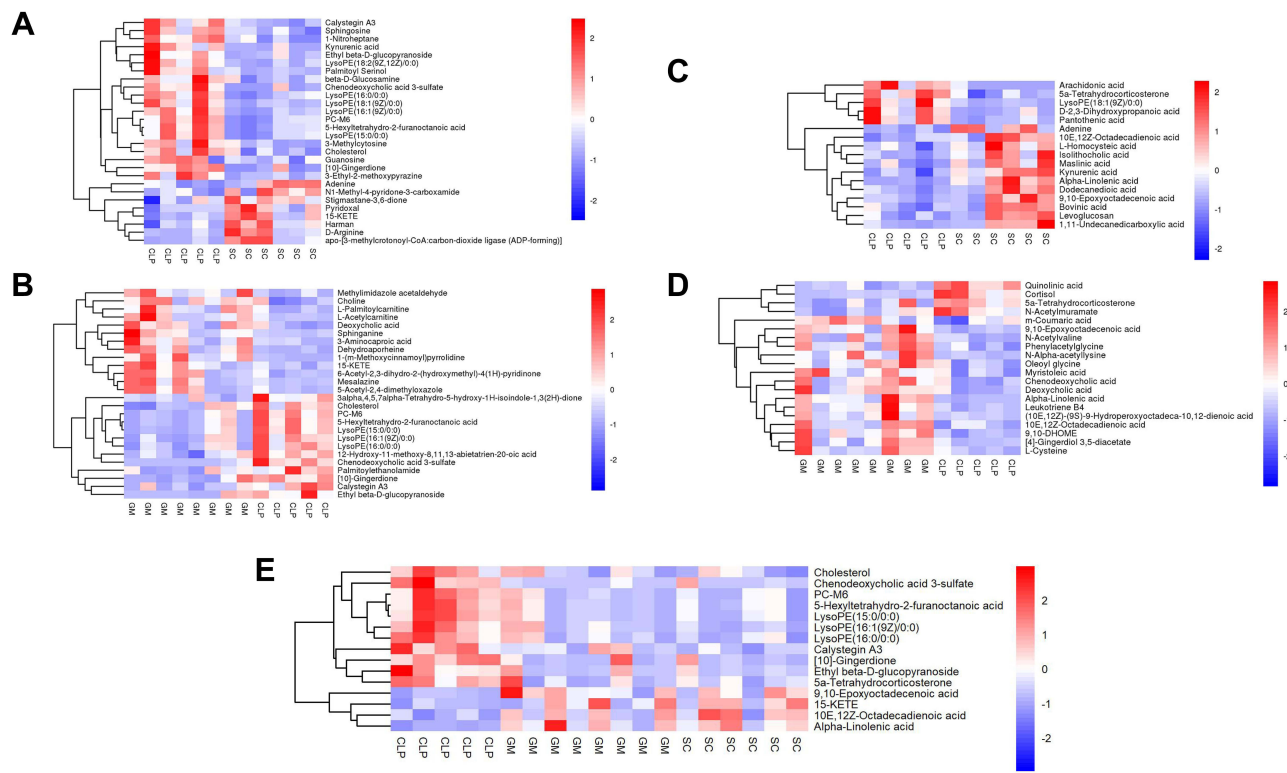
Figure 4 Heatmap of fecal differential metabolites in positive and negative ion mode. Red indicates highly expressed, and blue indicates expressed at a low level. (**A**) SC and CLP group (positive ion mode). (**B**) GM group and CLP group (positive ion mode). (**C**) SC and CLP group (negative ion mode). (**D**) GM group and CLP group (negative ion mode). (**E**) Heatmap of common differential metabolites of the three groups.

significantly changed metabolites in the SC, CLP, and GM groups. The detailed information of each metabolite is shown in Table 2. As shown in Figure 4E, 15 metabolites are mainly divided into 11 fatty acids and 4 other classified metabolites, namely, 10E, 12Z-octadecadienoic acid, 9,10-epoxyoctadecenoic acid, 15-KETE, and alpha-linolenic acid. These four fatty acids are grouped together, and the relative abundance is lower in the CLP group but higher in SC and GM groups.

Table 2 Detailed Information of Differential Metabolites of the SC, CLP, and GM Groups (VIP > 1, P < 0.05)

Differential Metabolites	RT	m/z	VIP	Fold Change (CLP/SC)	Fold Change (CLP/GM)	Classification
[10]-Gingerdione	79.03	349.23	1.78	3.40	2.98	1
PC-M6	225.00	422.27	1.58	3.11	2.79	2
Calystegin A3	291.51	160.10	1.73	2.80	1.93	3
LysoPE (16:1(9Z)/0:0)	224.04	452.28	1.85	4.90	2.49	4
LysoPE (16:0/0:0)	222.75	454.30	1.25	3.77	0.19	4
5-Hexyltetrahydro-2-furanoctanoic acid	224.98	299.26	1.58	3.08	2.82	4
Cholesterol	25.57	369.35	1.39	2.08	1.72	4
LysoPE (15:0/0:0)	224.99	440.28	1.61	3.11	2.89	4
15-KETE	254.16	336.25	1.42	0.33	0.36	4
Chenodeoxycholic acid 3-sulfate	281.50	473.26	1.83	6.31	17.54	4
Ethyl beta-D-glucopyranoside	292.10	209.10	1.81	4.71	3.19	5
10E,12Z-Octadecadienoic acid	40.63	279.23	1.30	0.46	0.57	4
Alpha-Linolenic acid	43.74	277.22	1.92	0.34	0.33	4
9,10-Epoxyoctadecenoic acid	48.03	295.23	1.37	0.48	0.41	4
5a-Tetrahydrocorticosterone	146.75	349.24	1.05	2.44	-	4

Notes: VIP, contribution rate of different substances to orthogonal partial least squares discriminant analysis (OPLS-DA) model construction. Classification: 1. Benzenoids; 2. Organoheterocyclic compounds; 3. Alkaloids and derivatives; 4. Lipids and lipid-like molecules; 5. Organic oxygen compounds.
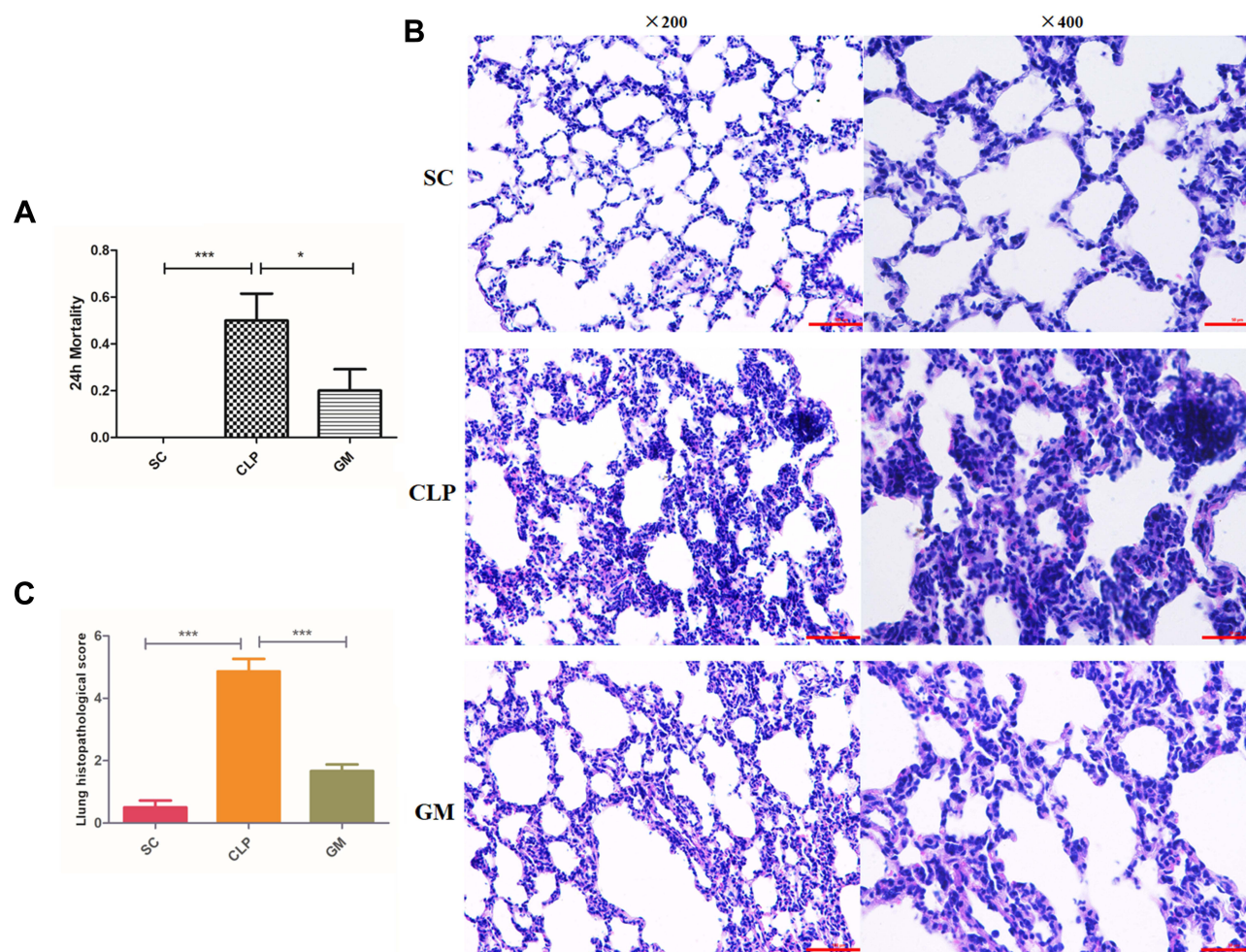**Abbreviation**: RT, retention time.

Metabolic Pathway Analysis of Key Differential Metabolites

Using MetaboAnalyst 3.0 and the KEGG database, the different metabolite pathways between the CLP and GM groups were analyzed. It was found that GM mainly regulates sphingolipid metabolism, histidine metabolism, steroid biosynthesis, glycerophospholipid metabolism, primary bile acid biosynthesis, and alpha-linolenic acid metabolism (Supplementary Figure 9). They are consistent with the predicted pathway of Tax4Fun function, and the GM group was negatively related to apoptosis, lipopolysaccharide biosynthesis, steroid hormone biosynthesis, and sphingolipid metabolism. Therefore, changes in gut metabolites after GM application may be related to gut microbiota dysbiosis.

Links Between Different Genera and Metabolites

To further investigate the microbiota–intestinal metabolite relationship after GM application, Spearman correlation analysis was used to determine the connections between 27 different intestinal genera and differential metabolites between the CLP and GM groups. Some CLP-rich genera (Akkermansia and Escherichia–Shigella) were positively associated with Cortisol and Palmitoylethanolamide, and negatively correlated with Choline, Deoxycholic acid, 10E,12Z-Octadecadienoic acid, Chenodeoxycholic acid, [4]-Gingerdiol 3,5-diacetate, Oleoyl glycine and 9,10-Epoxyoctadecenoic acid. Moreover, the GM-rich genus (Lactobacillus, Pygmaiobacter and Erysipelotrichaceae_UCG-003) were positively associated with Deoxycholic acid and Chenodeoxycholic acid, and negatively correlated with Calystegin A3, Palmitoylethanolamide, [10]-Gingerdione, 12-Hydroxy-11-methoxy-8,11,13-abietatrien-20-oic acid. Notably, these 3 metabolites (Palmitoylethanolamide, Deoxycholic acid and Chenodeoxycholic acid) have significant correlation with CLP- genus (Akkermansia and Escherichia–Shigella) and GM-rich genus (Lactobacillus, Pygmaiobacter and Erysipelotrichaceae_UCG-003) (Figure 5).

Figure 5 Heatmap between different genera of intestinal microbiota and metabolites in CLP and GM groups. Red, positive correlation; blue, negative correlation. × mean $P < 0.05$. (**A**) Positive ion mode. (**B**) Negative ion mode.

Figure 6 (**A**) The mortality rate in the SC, CLP, and GM groups at 24 h after operation; Comparison with CLP, *$P < 0.05$, ***$P < 0.001$. (**B**) The histopathological section of the lung tissue in the SC, CLP, and GM groups, respectively (bar = 100 μm). (**C**) The lung histopathological scores in the SC, CLP, and GM groups; Comparison with CLP, ***$P < 0.001$.

Effects of GM on Lung Damage and Survival in Rats with Sepsis

The mortality rate in the CLP group (10/20) at 24 h after operation was higher than in the SC group (0/20) ($P < 0.001$) and GM group (4/20) ($P < 0.05$) (Figure 6A). Lung histopathological scores were conducted according to Osman criteria,[40] and inflammatory infiltration, edema, and structural damage of the lung tissue in the CLP group were significantly worse than those in SC ($P < 0.001$) and GM ($P < 0.001$) groups (Figure 6B and C).

Discussion

The study demonstrates that GM could attenuate sepsis-related lung injury and reduce sepsis mortality by modulating the gut microbiota and its metabolites in septic rats. The abundance of gut microbiota associated with SCFA production and metabolites related to bile acid metabolism were all increased in GM-treated septic rats. Besides, the alterations in the gut microbiota of GM were significantly correlated with these metabolites. Our study supports the possibility of GM in sepsis treatment because GM protects against acute lung injury in sepsis.

The gut microbiota could prevent the colonization of intestinal pathogens, and studies have shown that impaired gastrointestinal function in sepsis leads to significant changes in intestinal flora, manifested as dysbacteriosis.[41,42] Studies have found that infiltrating neutrophils and other immune cells can release proteolytic enzymes and activate PAR, resulting in distribution changes of tight junction-related proteins, such as ZO-1 and occludins.[43] The intestinal epithelial barrier integrity is disrupted[44], promoting harmful bacteria into the systemic circulation and resulting in the imbalance of

gut microbiota.[45] Mice with high proteolytic activity had higher intestinal permeability and lower relative abundance of gut microbiota.[45] Theoretically, inhibition of serine proteases could alleviate disruption of intestinal homeostasis and have beneficial effects. Previous studies have shown that another serine protease inhibitor, ulinastatin, protects the integrity and function of the intestinal barrier in sepsis, reducing leakage of gut bacteria.[46] GM also can inhibit the function of various serine proteins and activated neutrophils, the production of PAR-2 and leukocyte adhesion molecules to reduce sepsis-induced inflammation. In this study, we observed an increase in the abundance of Lactobacillus, Pygmaiobacter and Erysipelotrichaceae_UCG-003 after GM treatment. Lactobacillus as a natural gastrointestinal flora have various beneficial effects, including interference with intestinal pathogens, maintaining gut barrier and regulating mucosal and systemic immune responses.[47] It was widely used in the prevention of *Clostridium difficile* infection.[48] And recent studies found Lactobacillus significantly improved intestinal dysbiosis,[49] reduced the risk of late-onset sepsis.[50] In addition, both Pygmaiobacter and Erysipelotrichaceae_UCG_003 are the main bacteria producing butyric acid, which is a type of SCFA.[51,52] And SCFAs are potent anti-inflammatory substances involved in mediating immune responses and inducing the formation of regulatory T cells in sepsis.[53,54] Therefore, GM-enriched genera contribute to gut microbiota homeostasis and regulate the inflammatory response. Besides, compared to CLP group, the Escherichia–Shigella and Akkermansia were significantly reduced in GM group. Escherichia–Shigella as a common pathogenic bacteria can promote the production of LPS[55] and induce macrophage death.[56] Interestingly, Akkermansia was considered to be a new generation probiotic, but it was significantly reduced after the use of GM. However, it has been reported that excessive Akkermansia can disrupt host mucins, increase intestinal permeability,[57] induce inflammation and promote colon tumorigenesis.[58,59] Increased Akkermansia abundance and decreased SCFA-producing bacteria also aggravate colorectal cancer.[60] Additionally, Seibert et al found that Akkermansia abundance was significantly increased at peak viral infection and allergic diseases,[61,62] which was also consistent with our findings.

The gut microbiota synthesizes, regulates and degrades a variety of metabolites as functional supplements for host metabolism, especially for dietary components that cannot be metabolized by the host.[63] Nearly 10% of metabolites in blood and more than 50% of metabolites in feces and urine originate from or are modified by gut microbiota.[64,65] Microbial products, such as SCFAs, may influence host metabolism by regulating appetite, lipogenesis, glucongenesis, inflammation, and other functions.[66] A byproduct of intestinal metabolism, bile acids are known to regulate hepatic metabolism,[67] which are also important for clearing bacteria and metabolic adaptation to inflammation in sepsis.[68] Deoxycholic acid activates the G protein-coupled receptor (TGR5), which affects neuroinflammation, cognitive or behavioral and became a therapeutic target for neurological outcomes in sepsis survivors.[69] Cholestasis is a common complication of sepsis, and elevated plasma Chenodeoxycholic acid levels predict sepsis-related mortality.[70] The Chenodeoxycholic acid derivative obeticholic acid could improve bile acid homeostasis and inhibit levels of inflammatory cytokines, which indicated bile acids were protective against sepsis.[71] Our study found that both deoxycholic acid and chenodeoxycholic acid were markly increased after treatment with GM, but Palmitoylethanolamide was decreased. Palmitoylethanolamide is an endogenous fatty acid amide that selectively activates peroxisome proliferator-activated receptor α (PPARα). Oxidation of fatty acids under starvation or fasting conditions stimulates transcription of PPARα-regulated genes and activates the oxidative system.[72] PPARγ is mainly involved in the regulating energy balance and lipid biosynthesis. Among them, the PPARγ2 isoform, as a receptor of 9, 10-DHOME, can prevent lipotoxicity through different mechanisms and enhance the lipid buffering capacity of liver and muscle.[73] This may be the reason why 9, 10-DHOME was significantly increased and Palmitoylethanolamide was decreased after GM treatment. Taken together, the improved survival rate of septic rats treated with GM may be attributed to changes in metabolites. However, the mechanisms underlying GM-induced changes in metabolite remain to be investigated.

Our study is the first to elucidate the relationship between intestinal microbiota and metabolomics after GM administration in sepsis. However, the study also has some limitations. First, the experiments had a small sample size, and the research results need to be verified with more animal experiments and clinical studies. In addition, we did not use pseudo-germ-free mice and fecal microbiota transplantation to verify a cause-consequence between microbiota and sepsis. Furthermore, although the effect of GM on lung damage using HE-stained sections was observed, a more complete experimental design is needed to explore the molecular mechanism by which GM improves sepsis prognosis.

In conclusion, this is the first study to elucidate that GM may improve sepsis-related lung injury and regulate gut microbiota and related metabolites, which provided a new idea for the treatment of sepsis.

Data Sharing Statement

The datasets used and/or analysed in the present study are available from the corresponding author on reasonable request.

Ethical Approval and Consent to Participate

All animal experiments were conducted according to the guidelines established by the National Institutes of Health (http://grants1.nih.gov/grants/olaw/) and approved by the Ethics Committee of the First Affiliated Hospital of Zhengzhou University (Approval No. 2019-KY-235).

Author Contributions

All authors made a significant contribution to the work reported, whether that is in the conception, study design, execution, acquisition of data, analysis and interpretation, or in all these areas; took part in drafting, revising or critically reviewing the article; gave final approval of the version to be published; have agreed on the journal to which the article has been submitted; and agree to be accountable for all aspects of the work.

Funding

Disclosure

The authors have no conflicts of interest to disclose.

References

1. Singer M, Deutschman CS, Seymour CW, et al. The third international consensus definitions for sepsis and septic shock (sepsis-3). *JAMA*. 2016;315(8):801–810. doi:10.1001/jama.2016.0287
2. Sun J, Ding X, Sun T. Mesenchymal stem cells in sepsis: from basic research to clinical application. *Intensive Care Res*. 2021;1(1–2):2–10. doi:10.2991/icres.k.210622.001
3. Fleischmann-Struzek C, Mellhammar L, Rose N, et al. Incidence and mortality of hospital- and ICU-treated sepsis: results from an updated and expanded systematic review and meta-analysis. *Intensive Care Med*. 2020;46(8):1552–1562. doi:10.1007/s00134-020-06151-x
4. Evans L, Rhodes A, Alhazzani W, et al. Surviving sepsis campaign: international guidelines for management of sepsis and septic shock 2021. *Intensive Care Med*. 2021;47(11):1181–1247. doi:10.1007/s00134-021-06506-y
5. Zheng MH, Bai JL, Meng MB, et al. Gabexate mesylate in the prevention of post-endoscopic retrograde cholangiopancreatography pancreatitis: a systematic review and meta-analysis update. *Curr Ther Res Clin Exp*. 2008;69(4):288–304. doi:10.1016/j.curtheres.2008.08.001
6. Yoo YW, Cha SW, Kim A, et al. The use of gabexate mesylate and ulinastatin for the prevention of post-endoscopic retrograde cholangiopan-creatography pancreatitis. *Gut Liver*. 2012;6(2):256–261. doi:10.5009/gnl.2012.6.2.256
7. Akahoshi T, Sugimori H, Kaku N, et al. Comparison of recombinant human thrombomodulin and gabexate mesylate for treatment of disseminated intravascular coagulation (DIC) with sepsis following emergent gastrointestinal surgery: a retrospective study. *Eur J Trauma Emerg Surg*. 2015;41 (5):531–538. doi:10.1007/s00068-014-0478-4
8. Urano T, Ihara H, Suzuki Y, et al. Coagulation-associated enhancement of fibrinolytic activity via a neutralization of PAI-1 activity. *Semin Thromb Hemost*. 2000;26(1):39–42. doi:10.1055/s-2000-9801
9. Xiang M, Wu X, Jing H, et al. The impact of platelets on pulmonary microcirculation throughout COVID-19 and its persistent activating factors. *Front Immunol*. 2022;13:955654. doi:10.3389/fimmu.2022.955654
10. Oh SH, Lee HY, Ki YJ, et al. Gabexate mesilate ameliorates the neuropathic pain in a rat model by inhibition of proinflammatory cytokines and nitric oxide pathway via suppression of nuclear factor-κB. *Korean J Pain*. 2020;33(1):30–39. doi:10.3344/kjp.2020.33.1.30
11. Hidaka S, Iwasaka H, Hagiwara S, et al. Gabexate mesilate inhibits the expression of HMGB1 in lipopolysaccharide-induced acute lung injury. *J Surg Res*. 2011;165(1):142–150. doi:10.1016/j.jss.2009.05.039

12. Murakami K, Okajima K, Uchiba M, et al. Gabexate mesilate, a synthetic protease inhibitor, attenuates endotoxin-induced pulmonary vascular injury by inhibiting tumor necrosis factor production by monocytes. *Crit Care Med*. 1996;24(6):1047–1053. doi:10.1097/00003246-199606000-00027

13. Xie LB, Zeng DY, Wang XD, et al. Preconditioning with gabexate is superior to inosine for ameliorating acute renal ischemia-reperfusion injury in rats. *Transplant Proc*. 2014;46(1):40–45. doi:10.1016/j.transproceed.2013.10.037

14. Niehaus GD, Kimura R, Traber LD, et al. Administration of a synthetic antiprotease reduces smoke-induced lung injury. *J Appl Physiol*. 1990;69 (2):694–699. doi:10.1152/jappl.1990.69.2.694

15. Park I, Kim M, Choe K, et al. Neutrophils disturb pulmonary microcirculation in sepsis-induced acute lung injury. *Eur Respir J*. 2019;53 (3):1800786. doi:10.1183/13993003.00786-2018

16. Uchiba M, Okajima K, Kaun C, et al. Gabexate mesilate, a synthetic anticoagulant, inhibits the expression of endothelial leukocyte adhesion molecules in vitro. *Crit Care Med*. 2003;31(4):1147–1153. doi:10.1097/01.CCM.0000060005.48885.2B

17. Levi M, Van Der Poll T. Coagulation and sepsis. *Thromb Res*. 2017;149:38–44. doi:10.1016/j.thromres.2016.11.007

18. Tsai HJ, Ding C, Tsao CM, et al. Effects of gabexate mesilate on coagulopathy and organ dysfunction in rats with endotoxemia: a potential use of thrombelastography in endotoxin-induced sepsis. *Blood Coagul Fibrinolysis*. 2015;26(2):175–184. doi:10.1097/MBC.0000000000000214

19. Lee YT, Wei J, Chuang YC, et al. Successful treatment with continuous enteral protease inhibitor in a patient with severe septic shock. *Transplant Proc*. 2012;44(3):817–819. doi:10.1016/j.transproceed.2012.03.032

20. Imhann F, Vich Vila A, Bonder MJ, et al. Interplay of host genetics and gut microbiota underlying the onset and clinical presentation of inflammatory bowel disease. *Gut*. 2018;67(1):108–119. doi:10.1136/gutjnl-2016-312135

21. Li H, Zhai R, Liang H, et al. [Analysis of the changes in intestinal microecology in the early stage of sepsis rat based on 16S rDNA sequencing]. *Zhonghua Wei Zhong Bing Ji Jiu Yi Xue*. 2022;34(1):28–34. Chinese. doi:10.3760/cma.j.cn121430-20201215-00754

22. Dickson RP. The microbiome and critical illness. *Lancet Respir Med*. 2016;4(1):59–72. doi:10.1016/S2213-2600(15)00427-0

23. Liu W, Cheng M, Li J, et al. Classification of the gut microbiota of patients in intensive care units during development of sepsis and septic shock. *Genomics Proteomics Bioinformatics*. 2020;18(6):696–707. doi:10.1016/j.gpb.2020.06.011

24. Wang C, Li Q, Tang C, et al. Characterization of the blood and neutrophil-specific microbiomes and exploration of potential bacterial biomarkers for sepsis in surgical patients. *Immun Inflamm Dis*. 2021;9(4):1343–1357. doi:10.1002/iid3.483

25. Du B, Shen N, Tao Y, et al. Analysis of gut microbiota alteration and application as an auxiliary prognostic marker for sepsis in children: a pilot study. *Transl Pediatr*. 2021;10(6):1647–1657. doi:10.21037/tp-21-51

26. Dang AT, Marsland BJ. Microbes, metabolites, and the gut–lung axis. *Mucosal Immunol*. 2019;12(4):843–850. doi:10.1038/s41385-019-0160-6

27. Brown RL, Sequeira RP, Clarke TB. The microbiota protects against respiratory infection via GM-CSF signaling. *Nat Commun*. 2017;8(1):1512. doi:10.1038/s41467-017-01803-x

28. Chunxi L, Haiyue L, Yanxia L. The gut microbiota and respiratory diseases: new evidence. *J Immunol Res*. 2020;2020:2340670. doi:10.1155/2020/2340670

29. Roduit C, Frei R, Ferstl R, et al. High levels of butyrate and propionate in early life are associated with protection against atopy. *Allergy*. 2019;74 (4):799–809. doi:10.1111/all.13660

30. Cait A, Hughes MR, Antignano F, et al. Microbiome-driven allergic lung inflammation is ameliorated by short-chain fatty acids. *Mucosal Immunol*. 2018;11(3):785–795. doi:10.1038/mi.2017.75

31. Antunes KH, Fachi JL, De Paula R, et al. Microbiota-derived acetate protects against respiratory syncytial virus infection through a GPR43-type 1 interferon response. *Nat Commun*. 2019;10(1):3273. doi:10.1038/s41467-019-11152-6

32. Sencio V, Barthelemy A, Tavares LP, et al. Gut dysbiosis during influenza contributes to pulmonary pneumococcal superinfection through altered short-chain fatty acid production. *Cell Rep*. 2020;30(9):2934–2947.e6. doi:10.1016/j.celrep.2020.02.013

33. Wu T, Li H, Su C, et al. Microbiota-derived short-chain fatty acids promote LAMTOR2-mediated immune responses in macrophages. *mSystems*. 2020;5:6. doi:10.1128/mSystems.00587-20

34. Wu T, Xu F, Su C, et al. Alterations in the gut microbiome and cecal metabolome during Klebsiella pneumoniae-induced pneumosepsis. *Front Immunol*. 2020;11:1331. doi:10.3389/fimmu.2020.01331

35. Ebrahimi-Mameghani M, Sanaie S, Mahmoodpoor A, et al. Effect of a probiotic preparation (VSL#3) in critically ill patients: a randomized, double-blind, placebo-controlled trial (pilot study). *Pak J Med Sci*. 2013;29(2):490–494. doi:10.12669/pjms.292.3370

36. Gai X, Wang H, Li Y, et al. Fecal microbiota transplantation protects the intestinal mucosal barrier by reconstructing the gut microbiota in a murine model of sepsis. *Front Cell Infect Microbiol*. 2021;11:736204. doi:10.3389/fcimb.2021.736204

37. Cui Y, Liu S, Zhang X, et al. Metabolomic analysis of the effects of adipose-derived mesenchymal stem cell treatment on rats with sepsis-induced acute lung injury. *Front Pharmacol*. 2020;11:902. doi:10.3389/fphar.2020.00902

38. Liang H, Ding X, Yu Y, et al. Adipose-derived mesenchymal stem cells ameliorate acute liver injury in rat model of CLP induced-sepsis via sTNFR1. *Exp Cell Res*. 2019;383(1):111465. doi:10.1016/j.yexcr.2019.06.010

39. Segata N, Izard J, Waldron L, et al. Metagenomic biomarker discovery and explanation. *Genome Biol*. 2011;12(6):R60. doi:10.1186/gb-2011-12-6-r60

40. Osman MO, Kristensen JU, Jacobsen NO, et al. A monoclonal anti-interleukin 8 antibody (WS-4) inhibits cytokine response and acute lung injury in experimental severe acute necrotising pancreatitis in rabbits. *Gut*. 1998;43(2):232–239. doi:10.1136/gut.43.2.232

41. Haak BW, Levi M, Wiersinga WJ. Microbiota-targeted therapies on the intensive care unit. *Curr Opin Crit Care*. 2017;23(2):167–174. doi:10.1097/MCC.0000000000000389

42. Sun T, Wang L, Zhang H. Intestinal microbiota in sepsis. *Intensive Care Res*. 2022;2(1–2):1–7. doi:10.1007/s44231-022-00001-8

43. Mariaule V, Kriaa A, Soussou S, et al. Digestive inflammation: role of proteolytic dysregulation. *Int J Mol Sci*. 2021;22:6. doi:10.3390/ijms22062817

44. Dabek M, Ferrier L, Annahazi A, et al. Intracolonic infusion of fecal supernatants from ulcerative colitis patients triggers altered permeability and inflammation in mice: role of cathepsin G and protease-activated receptor-4. *Inflamm Bowel Dis*. 2011;17(6):1409–1414. doi:10.1002/ibd.21454

45. Allam-Ndoul B, Castonguay-Paradis S, Veilleux A. Gut microbiota and intestinal trans-epithelial permeability. *Int J Mol Sci*. 2020;21(17):6402. doi:10.3390/ijms21176402

46. Jiang L, Yang L, Zhang M, et al. Beneficial effects of ulinastatin on gut barrier function in sepsis. *Indian J Med Res*. 2013;138(6):904–911.

47. Madsen K. Probiotics in critically ill patients. *J Clin Gastroenterol*. 2008;42:S116–8. doi:10.1097/MCG.0b013e31817283cb

48. Goldstein EJ, Tyrrell KL, Citron DM. Lactobacillus species: taxonomic complexity and controversial susceptibilities. *Clin Infect Dis*. 2015;60 (Suppl 2):S98–107. doi:10.1093/cid/civ072

49. Shimizu K, Yamada T, Ogura H, et al. Synbiotics modulate gut microbiota and reduce enteritis and ventilator-associated pneumonia in patients with sepsis: a randomized controlled trial. *Crit Care*. 2018;22(1):239. doi:10.1186/s13054-018-2167-x

50. Robertson C, Savva GM, Clapuci R, et al. Incidence of necrotising enterocolitis before and after introducing routine prophylactic Lactobacillus and Bifidobacterium probiotics. *Arch Dis Child Fetal Neonatal Ed*. 2020;105(4):380–386. doi:10.1136/archdischild-2019-317346

51. Yang G, Xu C, Varjani S, et al. Metagenomic insights into improving mechanisms of Fe(0) nanoparticles on volatile fatty acids production from potato peel waste anaerobic fermentation. *Bioresour Technol*. 2022;361:127703. doi:10.1016/j.biortech.2022.127703

52. Liu S, Li E, Sun Z, et al. Altered gut microbiota and short chain fatty acids in Chinese children with autism spectrum disorder. *Sci Rep*. 2019;9 (1):287. doi:10.1038/s41598-018-36430-z

53. Sivaprakasam S, Gurav A, Paschall AV, et al. An essential role of Ffar2 (Gpr43) in dietary fibre-mediated promotion of healthy composition of gut microbiota and suppression of intestinal carcinogenesis. *Oncogenesis*. 2016;5(6):e238. doi:10.1038/oncsis.2016.38

54. Liu H, Wang J, He T, et al. Butyrate: a double-edged sword for health?. *Adv Nutr*. 2018;9(1):21–29. doi:10.1093/advances/nmx009

55. Sun J, Ding X, Liu S, et al. Adipose-derived mesenchymal stem cells attenuate acute lung injury and improve the gut microbiota in septic rats. *Stem Cell Res Ther*. 2020;11(1):384. doi:10.1186/s13287-020-01902-5

56. Wang W, Chen Q, Yang X, et al. Sini decoction ameliorates interrelated lung injury in septic mice by modulating the composition of gut microbiota. *Microb Pathog*. 2020;140:103956. doi:10.1016/j.micpath.2019.103956

57. Nishiwaki H, Hamaguchi T, Ito M, et al. Short-chain fatty acid-producing gut microbiota is decreased in Parkinson's disease but not in rapid-eye-movement sleep behavior disorder. *mSystems*. 2020;5:6. doi:10.1128/mSystems.00797-20

58. Baxter NT, Zackular JP, Chen GY, et al. Structure of the gut microbiome following colonization with human feces determines colonic tumor burden. *Microbiome*. 2014;2:20. doi:10.1186/2049-2618-2-20

59. Ganesh BP, Klopfleisch R, Loh G, et al. Commensal Akkermansia muciniphila exacerbates gut inflammation in Salmonella Typhimurium-infected gnotobiotic mice. *PLoS One*. 2013;8(9):e74963. doi:10.1371/journal.pone.0074963

60. Zhang Z, Cao H, Song N, et al. Long-term hexavalent chromium exposure facilitates colorectal cancer in mice associated with changes in gut microbiota composition. *Food Chem Toxicol*. 2020;138:111237. doi:10.1016/j.fct.2020.111237

61. Seibert B, Cáceres CJ, Cardenas-Garcia S, et al. Mild and severe SARS-CoV-2 infection induces respiratory and intestinal microbiome changes in the K18-hACE2 transgenic mouse model. *Microbiol Spectr*. 2021;9(1):e0053621. doi:10.1128/Spectrum.00536-21

62. Yan X, Yan J, Xiang Q, et al. Fructooligosaccharides protect against OVA-induced food allergy in mice by regulating the Th17/Treg cell balance using tryptophan metabolites. *Food Funct*. 2021;12(7):3191–3205. doi:10.1039/D0FO03371E

63. Nicholson JK, Holmes E, Kinross J, et al. Host-gut microbiota metabolic interactions. *Science*. 2012;336(6086):1262–1267. doi:10.1126/science.1223813

64. Zheng X, Xie G, Zhao A, et al. The footprints of gut microbial-mammalian co-metabolism. *J Proteome Res*. 2011;10(12):5512–5522. doi:10.1021/pr2007945

65. Wikoff WR, Anfora AT, Liu J, et al. Metabolomics analysis reveals large effects of gut microflora on mammalian blood metabolites. *Proc Natl Acad Sci USA*. 2009;106(10):3698–3703. doi:10.1073/pnas.0812874106

66. Cuevas-Sierra A, Ramos-Lopez O, Riezu-Boj JI, et al. Diet, gut microbiota, and obesity: links with host genetics and epigenetics and potential applications. *Adv Nutr*. 2019;10(suppl_1):S17–s30. doi:10.1093/advances/nmy078

67. Hylemon PB, Zhou H, Pandak WM, et al. Bile acids as regulatory molecules. *J Lipid Res*. 2009;50(8):1509–1520. doi:10.1194/jlr.R900007-JLR200

68. Strnad P, Tacke F, Koch A, et al. Liver - guardian, modifier and target of sepsis. *Nat Rev Gastroenterol Hepatol*. 2017;14(1):55–66. doi:10.1038/nrgastro.2016.168

69. Jin P, Deng S, Tian M, et al. INT-777 prevents cognitive impairment by activating Takeda G protein-coupled receptor 5 (TGR5) and attenuating neuroinflammation via cAMP/ PKA/ CREB signaling axis in a rat model of sepsis. *Exp Neurol*. 2021;335:113504. doi:10.1016/j.expneurol.2020.113504

70. Hao H, Cao L, Jiang C, et al. Farnesoid X receptor regulation of the NLRP3 inflammasome underlies cholestasis-associated sepsis. *Cell Metab*. 2017;25(4):856–867.e5. doi:10.1016/j.cmet.2017.03.007

71. Xiong X, Ren Y, Cui Y, et al. Obeticholic acid protects mice against lipopolysaccharide-induced liver injury and inflammation. *Biomed Pharmacother*. 2017;96:1292–1298. doi:10.1016/j.biopha.2017.11.083

72. Rao MS, Papreddy K, Musunuri S, et al. Prevention/reversal of choline deficiency-induced steatohepatitis by a peroxisome proliferator-activated receptor alpha ligand in rats. *In Vivo*. 2002;16(2):145–152.

73. Medina-Gomez G, Gray SL, Yetukuri L, et al. PPAR gamma 2 prevents lipotoxicity by controlling adipose tissue expandability and peripheral lipid metabolism. *PLoS Genet*. 2007;3(4):e64. doi:10.1371/journal.pgen.0030064